Journal of Hazardous Materials 162 (2009) 1249–1254

Contents lists available at ScienceDirect

Journal of Hazardous Materials

journal homepage: www.elsevier.com/locate/jhazmat

Low-temperature selective catalytic reduction of NO on MnO_x/TiO_2 prepared by different methods

Boqiong Jiang, Yue Liu, Zhongbiao Wu*

Department of Environmental Engineering, Zhejiang University, Hangzhou, Zhejiang Province 310027, China

ARTICLE INFO

Article history:
Received 23 April 2007
Received in revised form 2 April 2008
Accepted 9 June 2008
Available online 13 June 2008

Keywords:
MnO_x/TiO_2
Sol–gel
Impregnation
Coprecipitation
Interaction

ABSTRACT

Catalysts based on MnO_x/TiO_2 were prepared by sol–gel, impregnation, and coprecipitation methods for low-temperature selective catalytic reduction (SCR) of NO with NH_3. Among the catalysts, the sample prepared by sol–gel method had the best performance on both activity and SO_2 resistance. From the results of thermo gravimetric analysis (TGA), X-ray diffraction (XRD), transmission electron microscopy (TEM) and X-ray photoelectron spectrum (XPS), it was known that manganese oxides and titania existed in different phase in the samples prepared by three methods. Strong interaction, large surface area, high concentration of hydroxyl groups, high concentration of amorphous Mn on the surface might be the main reasons for the excellent performance of the catalysts.

1. Introduction

In recent years, there is an interest in developing a potential low-temperature (353–533 K) SCR catalyst, and then the catalyst bed can be moved downstream of the desulfurization scrubber and/or particulate control device, where most of sulfur dioxide and dust is removed and the deactivation is weakened.

Manganese oxides attract interest as catalysts since they contain various types of labile oxygen, which are necessary to complete a catalytic cycle. The activity and selectivity of pure manganese oxides in SCR have been intensively investigated by Kapteijn et al. [1], and 90% of NO conversion was obtained at 450 K. Furthermore, manganese oxides were based on several carriers to enhance the catalytic activity, such as Al_2O_3 [2], TiO_2 [3], CeO_2 [4] and so on. It was reported that the dispersion of the manganese oxides had important influence on the reaction, since crystalline manganese oxide contributed little to activity [5–7].

In previous studies, almost all of the manganese oxides catalysts studied for low-temperature SCR were prepared by solution impregnation method [3,8], and some were prepared by coprecipitation method [9]. As for sol–gel method, there were few studies reported on low-temperature SCR catalysts. However, in other field, this method was widely used as an effective one for catalyst preparation [10,11]. Therefore, sol–gel method could be an alternative method to prepare catalyst for low-temperature SCR. In this study, the sol–gel method was introduced to prepare the catalysts based on MnO_x/TiO_2 for low-temperature SCR. And the comparison of the activity and characterization of the catalysts prepared by different methods (sol–gel, impregnation and coprecipitation) were carried out. When the catalysts were prepared by sol–gel method, the particles could be well dispersed during the process of preparation, and the interaction was stronger, leading to lower crystallinity of the samples. For MnO_x/TiO_2(s), better nanostructure was obtained, and more manganese oxides could exist as amorphous phase.

2. Experimental

2.1. Catalyst preparation

2.1.1. Sol–gel method (s)

The catalyst was obtained by sol–gel method. All chemicals used were of analytical grade. Butyl titanate (0.1–0.3 mol), ethanol (0.8 mol), water (0.6 mol), acetic acid (0.3 mol), and manganese nitrate (0.04–0.12 mol) were mixed under vigorous stirring at 298 K formed transparent yellow sol. After stable at 298 K for several days, the sol transformed to gel. The gel was dried at 353 K, resulting in a porous solid. The obtained solid was crushed and sieved to 60–100 mesh, then calcined at 773 K for 6 h in air in a tubular furnace. The catalyst was denoted as $MnO_x(z)/TiO_2$, where z represents the mole ratio of Mn/Ti, e.g., $MnO_x(0.4)/TiO_2$.

* Corresponding author. Tel.: +86 571 87952459; fax: +86 571 87953088.
E-mail address: zbwu@zju.edu.cn (Z. Wu).

0304-3894/$ – see front matter © 2008 Elsevier B.V. All rights reserved.
doi:10.1016/j.jhazmat.2008.06.013

2.1.2. Impregnation method (i)

The catalysts were prepared by impregnation of TiO_2 (P25, supplier Degussa) with manganese nitrate. 20 ml of purified water by using a Milli-Q system was added to the beaker containing 4 g of support. The mixture was washed with purified water by using a Milli-Q system for several times, and then dried at 353 K for 6 h. The solid samples were crushed and sieved to 60–100 mesh, and then calcined at 773 K for 6 h.

2.1.3. Coprecipitation method (c)

For this method, certain amount of manganese nitrate and titanium sulphate was dissolved completely in 200 ml water, and then ammonia water was gradually added with thorough stirring. The mixture was stirred steadily for 2 h at 298 K and then filtered and washed with purified water by using a Milli-Q system for five times. The obtained samples were first dried at 353 K for 6 h, and were crushed and sieved to 60–100 mesh. Finally, the samples were calcined at 773 K for 6 h.

2.2. Activity measurement

The SCR activity measurement was carried out in a fixed-bed, stainless steel flow reactor. The experiments were performed under atmospheric pressure at 343–523 K. The reactor consisted of a steel tube of 1-cm i.d. in which 4 ml of catalyst was placed. The typical reactant gas composition was as follows: 1.222 g/m^3 NO (298 K), 0.693 g/m^3 NH_3 (298 K), 3% O_2, 0.522 g/m^3 SO_2 (298 K, when used), and balance N_2. The total flow rate was 2000 ml/min. The tubing of the reactor system was heat traced to prevent formation and deposition of ammonium nitrate and the reaction temperature was controlled by an OMRON programmable temperature controller. NO, NO_2, O_2 and SO_2 concentration were monitored by a flue gas analyzer (KM9106 Quintox Kane International Limited). For the reaction was carried out at low temperature, it must be confirmed that the decrease of NO was not caused by the adsorption of NO in the catalysts. Thus, at the beginning of each experiment, we purged the catalyst with reaction gas until the NO concentration of out gas reached the inlet gas concentration.

2.3. Characterization of the samples

Thermo gravimetric analysis (TGA) and differential scanning calorimetry analysis (DSC) for the different series of catalyst were carried out simultaneously in a Netzsch STA 409 instrument. X-ray diffraction (XRD) measurements were carried out with a XD-2 X-ray diffractometer using Cu Kα radiation. X-ray photoelectron spectrum (XPS) measurements were used to determine the atomic concentration and the state of the elements on catalyst surface with a V.G. Scientific Escalab 250 with Al Kα X-rays. The concentration of Mn, Ti and O on the surface of the samples was calculated from the integral of peak areas of the XPS data divided by each sensitivity factor of the element. Microstructures of the prepared samples were observed with a JOEL JEM-2010 electron microscope. Adsorbed-1 Quantachrom was used to calculate the surface area of the samples.

3. Results and discussion

3.1. Overview of the catalysts

Fig. 1 shows the NO conversion at 423 K by using the catalysts prepared by different methods. For each method, the variation of Mn loading had different effects on the catalytic activity. As we reported previously, the loading of Mn had significant effect on the activity of MnO_x/TiO_2(s). NO conversion increased with the increase of Mn loading until the ratio of Mn/Ti reached 0.4, and then the further increase of Mn loading would lead to the reduction of NO conversion because of the sintering effect [12]. When the catalysts were prepared by impregnation and/or coprecipitation method, the catalytic activity was not greatly influenced by the Mn loading. The similar results could be obtained from the work by Qi and Yang [8]. For all of the samples, $MnO_x(0.4)/TiO_2$(s) had the highest activity (92.6%) at 423 K, which was a little bit higher than that of the same type of catalyst prepared by impregnation method in the previous study [8]. This result is different from the photocatalytic investigation by using similar catalysts [13]. In the photocatalytic reaction, the activity was greatly influenced by light absorption and electron-hole generation, while in SCR reaction the influence parameter was different.

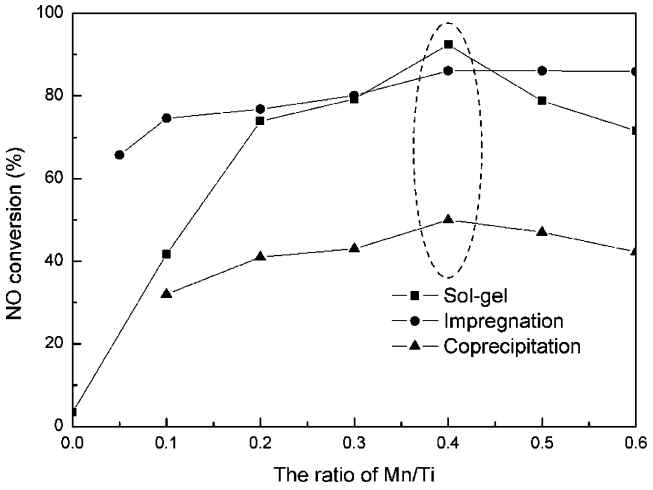

Fig. 1. The variation of the catalytic activity with different ratio of Mn/Ti at 423 K. Reaction conditions: [NO] = [NH_3] = 1000 ppm, [O_2] = 3%, balance N_2, total flow rate 2000 ml/min, and catalyst 4 ml.

When the ratio of Mn/Ti was 0.4, the activity of the catalysts prepared by three methods reached their highest value. Therefore, $MnO_x(0.4)/TiO_2$ was selected to be investigated for each method.

3.2. Characterization of the catalysts

XPS was used to measure the concentration of the atoms on the surface of $MnO_x(0.4)/TiO_2$(s), $MnO_x(0.4)/TiO_2$(i) and $MnO_x(0.4)/TiO_2$(c). When the three catalysts were prepared, the ratio of Mn/Ti was equal. However, as shown in Table 1, the concentration of Mn on the surface of $MnO_x(0.4)/TiO_2$(s) was highest, and the order of Mn/Ti ratio on the surface was $MnO_x(0.4)/TiO_2$(s) > $MnO_x(0.4)/TiO_2$(i) > $MnO_x(0.4)/TiO_2$(c). It was noted that the concentration of Mn in the three samples was in the same sequence of the catalytic activity. It might be because the higher concentration of Mn on the surface of the catalyst would result in higher reaction capacity of NO, contributing to better catalytic activity.

Typical TG and DSC curves for the three samples were shown in Fig. 2. It could be observed from Fig. 2(a) that there was continuous weight loss during the heating process for $MnO_x(0.4)/TiO_2$(s). The

Table 1
Atomic concentrations of three catalysts obtained with XPS

Catalyst	Metal content (at.%)			
	Mn	Ti	O	Mn/Ti
Mn(0.4)/TiO_2(s)	19.4	20.61	59.99	0.94
Mn(0.4)/TiO_2(i)	13.19	16.39	70.19	0.81
Mn(0.4)/TiO_2(c)	11.5	18.30	70.43	0.63

initial weight loss from 300 to 380 K could be related to the withdrawal of solvent residues and/or unbound stabilizing acid from the sample. The weight loss from 480 to 550 K was companied with a broad band in the DSC curve. It might be due to the formation of manganese oxides [14]. When the temperature achieved 820 K, an endothermic peak appeared in DSC curve, which corresponded to the formation of anatase form of TiO_2 and dehydroxylation of structural hydroxyl groups [15]. In Fig. 2(b), there was no apparent weight loss in TG curve, and two broad peaks were visible in DSC curve. For $MnO_x(0.4)/TiO_2$(i) was prepared with P25, which had constant crystallization of TiO_2, the two board could be considered caused by the variation of the manganese oxides. In Fig. 2(c), the weight loss from 300 to 380 K was due to desorption of physically adsorbed water and ammonia. Another loss from 450 to 560 K accompanied with the band from in DSC form also corresponded to the formation of manganese oxides, as in Fig. 2(a) and (b). As in the curve of $MnO_x(0.4)/TiO_2$(s), there was also a band formed at 820 K in DSC curve, which could be attributed to the formation of anatase phase of TiO_2. However, when the temperature was over 850 K, another peak appeared, and partly overlapped the peak at 820 K. With the increasing of temperature, there was a sharp weight loss from 920 to 1100 K. And when the temperature was over 1023 K, the mass loss still appeared in the TG curve for the sample. It may be related to the particle size effect of the nano-powder at higher temperature [16].

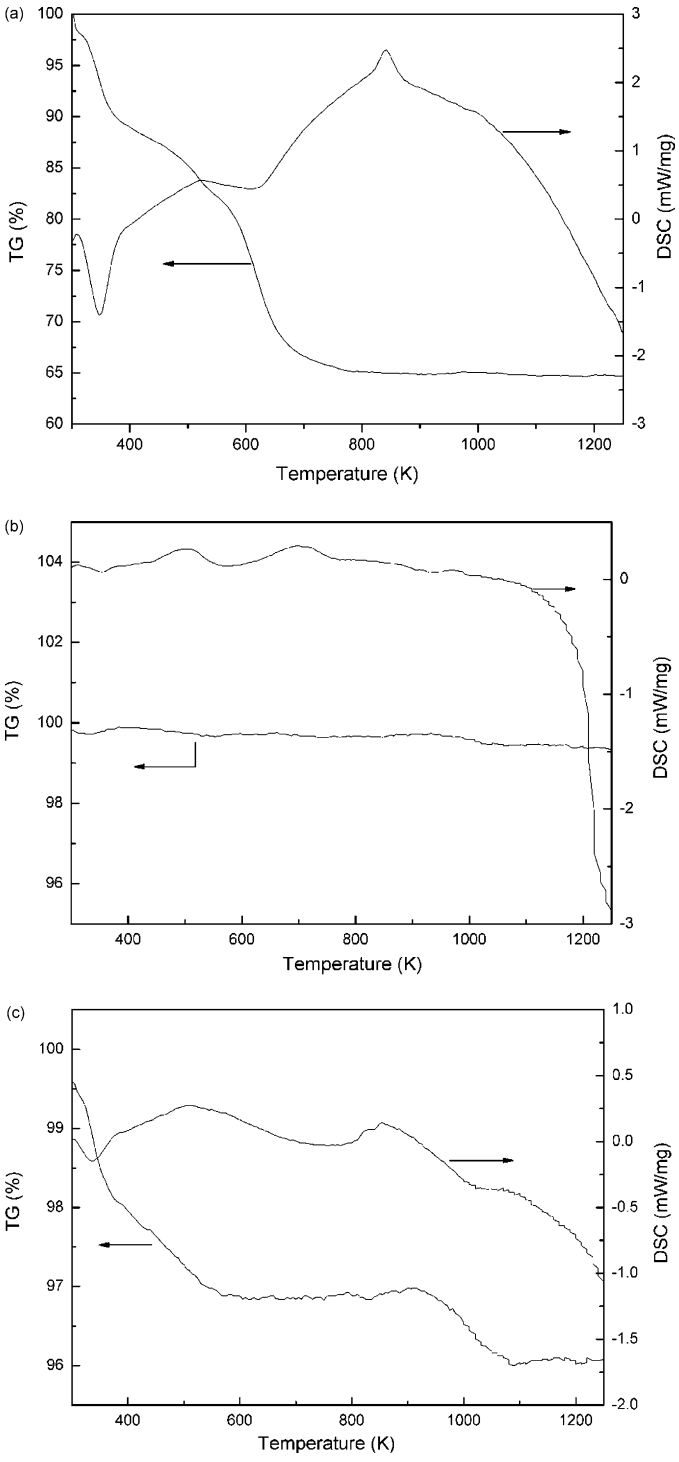

Fig. 2. TG-DSC analysis for three catalysts: (a) $Mn(0.4)/TiO_2$(s), (b) $Mn(0.4)/TiO_2$(i), and (c) $Mn(0.4)/TiO_2$(c).

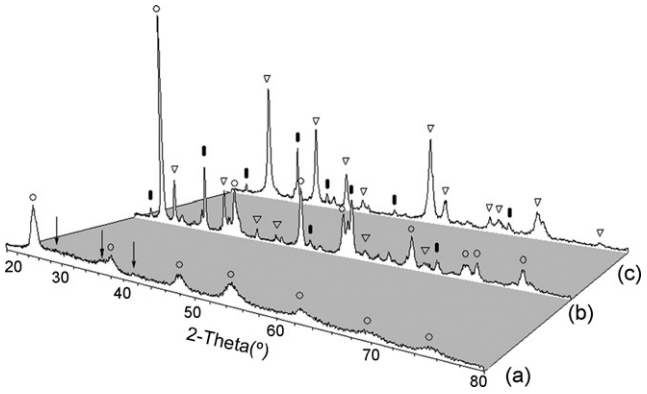

Fig. 3. XRD spectra of three catalysts: (a) $Mn(0.4)/TiO_2$(s), (b) $Mn(0.4)/TiO_2$(i), and (c) $Mn(0.4)/TiO_2$(c) ((○) anatase phase of TiO_2; (▽) rutile phase of TiO_2; (↓) MnO_2; (■) Mn_2O_3).

Fig. 3 shows the XRD patterns of the $MnO_x(0.4)/TiO_2$ catalysts for each method. From the XRD, it could be seen that the spectrum of $MnO_x(0.4)/TiO_2$(s) was simple. TiO_2 existed in anatase phase. Although several small peaks were apparent for crystalline MnO_2, the intensity of the bands was very low. Thus, it could be concluded that manganese oxides were dispersed well in this sample. For $MnO_x(0.4)/TiO_2$(i), there were two phases of TiO_2. Besides the anatase phase, several new peaks were apparent assigned to rutile

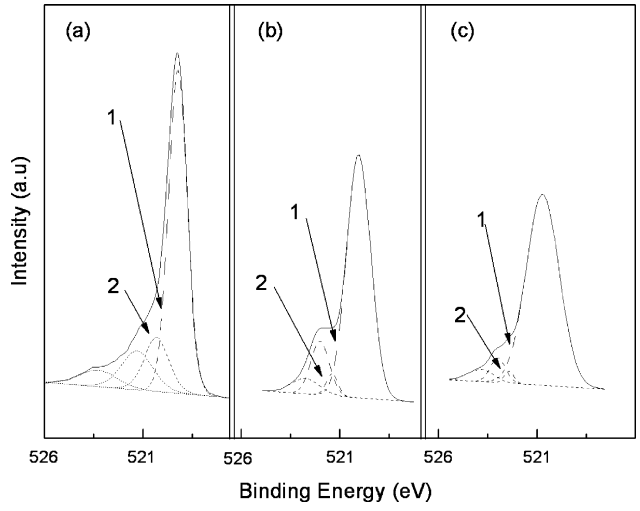

Fig. 4. O 1s XPS spectra for three catalysts: (a) $Mn(0.4)/TiO_2$(s), (b) $Mn(0.4)/TiO_2$(i), and (c) $Mn(0.4)/TiO_2$(c).

phase. There were no bands corresponded to MnO_2, and manganese oxides existed as Mn_2O_3 in the sample. For $MnO_x(0.4)/TiO_2$(c), the peaks for manganese oxides were consistent with that for $MnO_x(0.4)/TiO_2$(i). The DSC curve of $MnO_x(0.4)/TiO_2$(c) (Fig. 2 (c)) indicated that there was anatase phase of TiO_2 formed in this sample. However, in the XRD spectra, there was no peak attributed to anatase phase of TiO_2, and TiO_2 was present only in rutile phase. Therefore, the anatase phase of TiO_2 in this sample was not stable and easy to transform to rutile phase. It had been analyzed by Forzatti [17] that TiO_2 in anatase phase would be better carrier of the SCR catalyst. Thus, the existence of the rutile phase of TiO_2 in $MnO_x(0.4)/TiO_2$(c) might partly contribute to its low activity. Furthermore, in Fig. 3, the crystallinity of the $MnO_x(0.4)/TiO_2$(s) was lowest in the three samples. It implied that there were great interaction between TiO_2 and manganese oxides, and manganese oxides could well dispersed in the catalyst. In other two samples, besides the peaks of TiO_2, there were several apparent peaks due to crystalline phase of Mn_2O_3. Therefore, the interaction of Ti and Mn in these two samples was much weaker than in $MnO_x(0.4)/TiO_2$(s), and crystallinity of TiO_2 and Mn_2O_3 was very high. Therefore, the activities of $MnO_x(0.4)/TiO_2$(i) and $MnO_x(0.4)/TiO_2$(c) are lower than that of $MnO_x(0.4)/TiO_2$(s), since amorphous manganese oxide contribute more to NO conversion [3,7].

Besides of the investigation of the crystallization of Mn and Ti, the oxygen on the surface of the three samples was studied by XPS. The O 1s XPS spectra for the three catalysts were presented in Fig. 4. For all of the samples, the O 1 s spectrum was composed of four overlapping peaks. Peak 1 was around 530 eV, which corresponded to the oxygen in metal oxides [18]. Peak 2 was due to the OH oxygen that linked to protons [19]. The mechanism suggested by Pena et al.

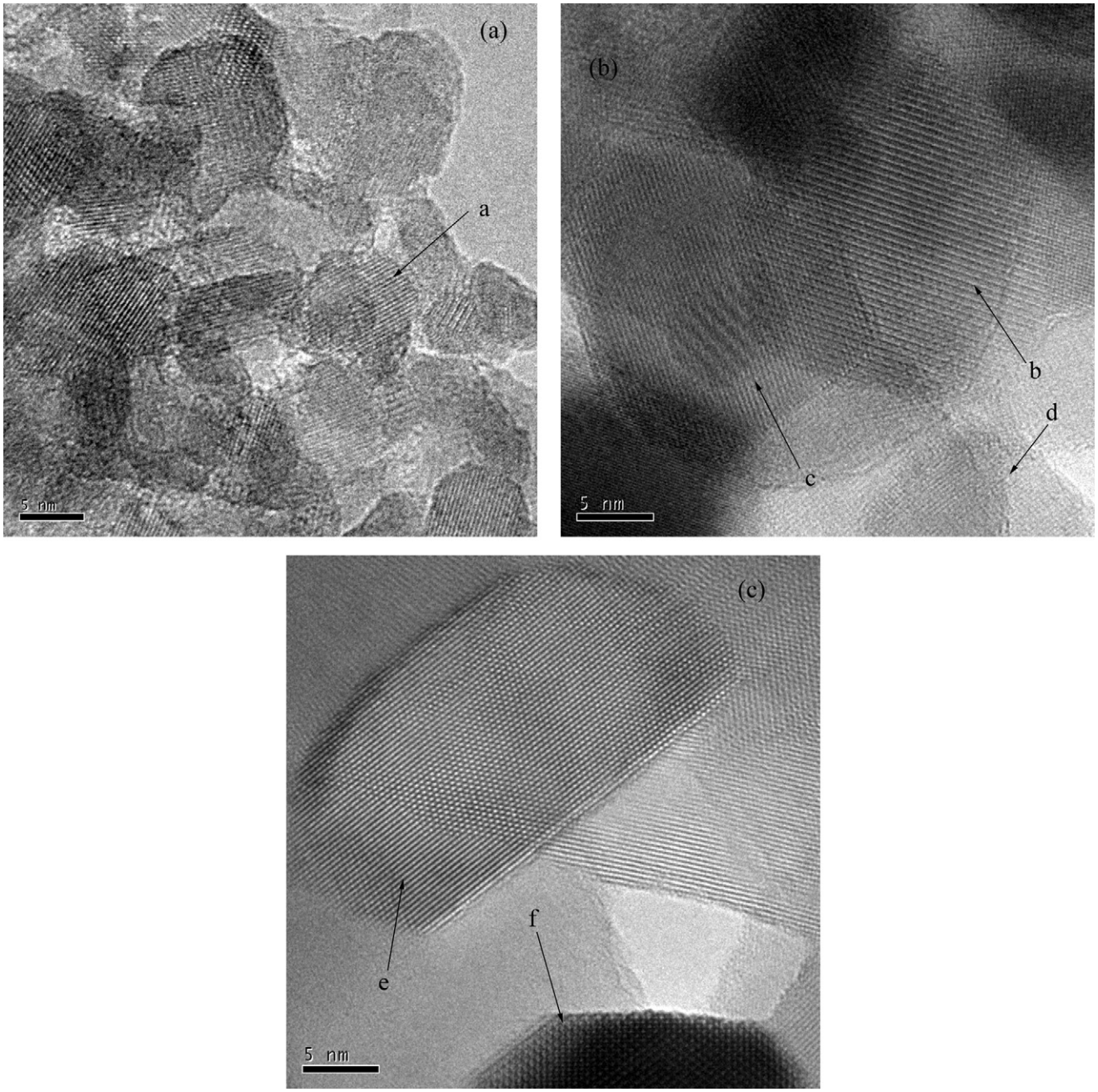

Fig. 5. HR-TEM micrographs of three catalysts: (a) Mn(0.4)/TiO_2(s), (b) Mn(0.4)/TiO_2(i), and (c) Mn(0.4)/TiO_2(c).

[20] showed the reaction commencing with the adsorption of NH_3 on the Lewis acid sites of Mn, which was formed from the oxygen and hydroxyl groups linked to Mn. Therefore, the hydroxyl group and the oxygen linked to Mn on the surface of the catalyst were important for SCR reaction. Although the oxygen concentration on the surface of $MnO_x(0.4)/TiO_2$(s) was much lower than other two samples (as shown in Table 1), it could be seen in Fig. 4 that on the surface of $MnO_x(0.4)/TiO_2$(s), the concentration of oxygen in metal oxides and hydroxyl groups was highest. It indicated that when the catalyst was used in SCR system, more Lewis acid sites could be supplied to promote the SCR reaction.

The microstructures and crystallization of the three samples were studied by HR-TEM (Fig. 5). As shown in Fig. 5(a), the crystal profiles were not very clear. The primary particle size of $MnO_x(0.4)/TiO_2$(s) was about 10 nm, and crystal TiO_2 or manganese oxides could not be seen. While in Fig. 5(b) and (c), the particle size was both more than 30 nm, and crystal TiO_2 could be apparently observed. These results indicated that there was much more crystalline phase of TiO_2 formed in the latter two samples, which was in good agreement with the XRD results. Furthermore, the different particle sizes of the three samples will result in their different surface areas. For $MnO_x(0.4)/TiO_2$(s), the Brunauer–Emmett–Teller (BET) surface area was determined to be 75.3 m^2/g, while for $MnO_x(0.4)/TiO_2$(i) and $MnO_x(0.4)/TiO_2$(c), the surface areas were 39.6 and 30.6 m^2/g, respectively. Thus, the smallest particle size of $MnO_x(0.4)/TiO_2$(s) had the highest surface area, which might be one of the main reasons for its highest catalytic activity.

In Fig. 5, the lattice fringes were observed on each sample, which could be used to identify the crystallographic spacing. In Fig. 5(a), the lattice fringes (a) was determined to be 0.347 nm, a little smaller than that of anatase phase (1 0 1) plane, and there were no plane observed corresponded to manganese oxides. Therefore, the manganese oxides were well dispersed and reduced the crystallinity of TiO_2. In Fig. 5(b), there were three kinds of lattice fringes. Fringe (b) was 0.479 nm, matched Mn_2O_3 (2 0 0). Fringe (c) and (d) was 0.352 and 0.321 nm, matched anatase (1 0 1) phase and rutile (1 1 0) phase of TiO_2, respectively. It could also be seen that the lattice fringe of Mn_2O_3 crossed that of TiO_2, indicating that Mn_2O_3 existed at the surface and covered TiO_2 in $MnO_x(0.4)/TiO_2$(i). In Fig. 5(c), there were two kinds of fringes: fringe (e) was about 0.326 nm and fringe (f) was about 0.384 nm, which matched rutile (1 1 0) phase of TiO_2 and Mn_2O_3 (2 1 1), respectively. There was no fringe due to anatase phase. The results agreed well with XRD.

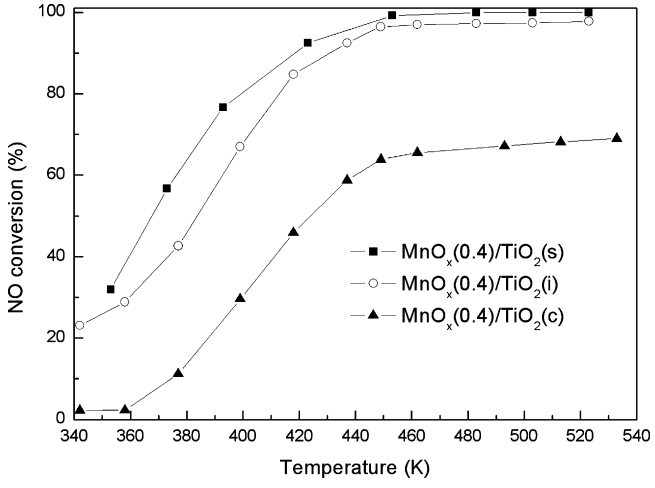

Fig. 6. The variation of the NO conversion for the three catalysts with temperature. Reaction conditions: [NO] = [NH_3] = 1000 ppm, [O_2] = 3%, balance N_2, total flow rate 2000 ml/min, and catalyst 4 ml.

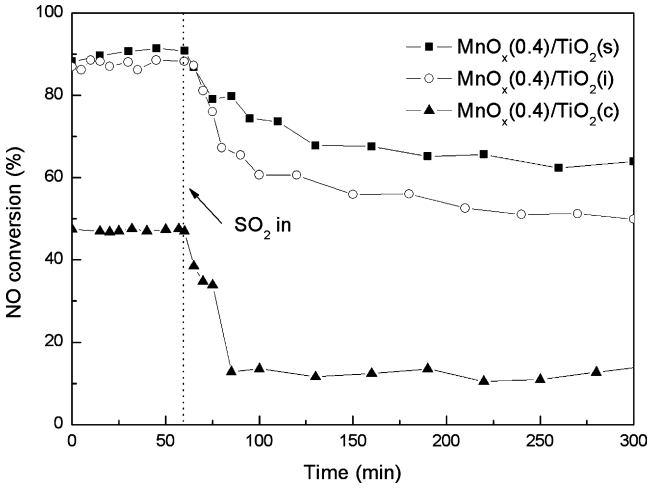

Fig. 7. The effect of SO_2 on NO conversion. Reaction conditions: [NO] = [NH_3] = 1000 ppm, [O_2] = 3%, [SO_2] = 200 ppm, balance N_2, total flow rate 2000 ml/min, and catalyst 4 ml.

3.3. Activity test

The activity of the three catalysts with the variation of temperature was presented in Fig. 6. It was clear that at low temperature, $MnO_x(0.4)/TiO_2$(s) performed most efficiently. More than 90% of the NO could be removed below 417 K. Accordingly, the temperature for $MnO_x(0.4)/TiO_2$(i) was about 432 K, and the NO conversion for $MnO_x(0.4)/TiO_2$(c) in the temperature window in the range of 423–473 K was below 60% all along. As reported by Tang et al. [21], the catalytic activity of manganese oxides catalyst was mainly affected by the oxidation state and crystallization. Combined with the results of XRD and HR-TEM, it could be known amorphous phase of manganese oxides and anatase phase of TiO_2 would contribute to good performance, while crystalline Mn_2O_3 and rutile phase of TiO_2 would lead to low activity. Therefore, when the catalyst was based on MnO_x/TiO_2, the catalytic activity was affected not only by the oxidation state and crystallinity of Mn, but also by the interaction between Mn and Ti.

It was known from previous study that SO_2 had strong inhibition effect on the catalytic activity [22,23]. Therefore, the effect of SO_2 was also investigated in this study. The influence of SO_2 on the NO conversion for $MnO_x(0.4)/TiO_2$ prepared by three methods at 423 K was shown in Fig. 7. When 200 ppm SO_2 was added to the system, the NO conversion for $MnO_x(0.4)/TiO_2$(s) changed from 90% to about 70% in 1 h at 423 K, and then NO conversion had little variation with time. For $MnO_x(0.4)/TiO_2$(i), the reduction of NO conversion was larger than on $MnO_x(0.4)/TiO_2$(s). And at the end of the period, NO conversion still decreased with time. When SO_2 was induced to $MnO_x(0.4)/TiO_2$(c), there was a sharp decrease of NO conversion from 48% to about 15% in 30 min, and then the NO conversion varied little with time. Therefore, it could be concluded that the catalyst prepared by sol–gel method had good resistance to SO_2. The behavior of the three samples was totally different, which might be due to the different groups formed on the surface, such as hydroxyl groups and NO complexes.

4. Conclusion

Catalysts based on MnO_x/TiO_2 were prepared by three different methods. Among the catalysts, $MnO_x(0.4)/TiO_2$ prepared by sol–gel method showed the highest activity for NO removal at low temperature. And it was also concluded that $MnO_x(0.4)/TiO_2$ prepared by sol–gel method presented higher resistant to SO_2. By using this

sample, 90% of NO could be removed at 417 K, and the NO conversion could be kept at 70% with 200 ppm SO_2 at 423 K. From the results of XPS, TG-DSC, XRD, BET area and HR-TEM, it was known that manganese oxides and TiO_2 existed in different phase for the catalysts prepared by different methods. Strong interaction, large surface area, high concentration of hydroxyl groups, high concentration of amorphous Mn on the surface might be the main reasons for the excellent performance of MnO_x/TiO_2 catalyst.

Acknowledgments

The project is financially supported by the National Natural Science Foundation of China (NSFC-20577040) and New Century Excellent Scholar Program of Ministry of Education of China (NCET-04-0549). The authors would also thank the support by Zhejiang University Joint Supervision Scheme with Hong Kong PolyU.

References

[1] F. Kapteijn, L. Singoredjo, A. Andreini, Activity and selectivity of pure manganese oxides in the selective catalytic reduction of nitric oxide with ammonia, Appl. Catal. B 3 (1994) 173–189.
[2] W.S. Kijlstra, D.S. Brands, E.K. Poels, A. Bliek, Mechanism of the selective catalytic reduction of NO with NH_3 over MnO_x/Al_2O_3. I. adsorption and desorption of the single reaction components, J. Catal. 171 (1997) 208–218.
[3] D.A. Pena, B.S. Uphade, P.G. Smirniotis, TiO_2-supported metal oxide catalysts for low-temperature selective catalytic reduction of NO with NH_3. I. evaluation and characterization of first row transition metals, J. Catal. 221 (2004) 421–431.
[4] M. Machida, D. Kurogi, T. Kijima, MnO_x–CeO_2 binary oxides for catalytic NO_x-sorption at low temperatures selective reduction of sorbed NO_x, Chem. Mater. 12 (2000) 3165–3170.
[5] G. Qi, R.T. Yang, Performance and kinetics study for low-temperature SCR of NO with NH_3 over MnO_x–CeO_2 catalyst, J. Catal. 217 (2003) 434–441.
[6] W.S. Kijlstra, D.S. Brands, H.I. Smit, E.K. Poels, A. Bliek, Mechanism of the selective catalytic reduction of NO with NH_3 over MnO_x/Al_2O_3. II. Reactivity of adsorbed NH_3 and NO complexes, J. Catal. 171 (1997) 219–230.
[7] H.Y. Huang, R.T. Yang, Removal of NO by reversible adsorption on Fe–Mn based transition metal oxides, Langmuir 17 (2001) 4997–5003.
[8] G. Qi, R.T. Yang, Low-temperature selective catalytic reduction of NO with NH_3 over iron and manganese oxides supported on titania, Appl. Catal. B 44 (2000) 217–225.
[9] G. Qi, R.T. Yang, R. Chang, MnO_x–CeO_2 mixed oxides prepared by co-precipitation for selective catalytic reduction of NO with NH_3 at low temperatures, Appl. Catal. B 51 (2004) 93–106.
[10] M. Keshmiri, M. Mohseni, T. Troczynski, Development of novel TiO_2 sol–gel-derived composite and its photocatalytic activities for trichloroethylene oxidation, Appl. Catal. B 53 (2004) 209–219.
[11] C. Su, B.Y. Hong, C.M. Tseng, Sol–gel preparation and photocatalysis of titanium dioxide, Catal. Today 96 (2004) 119–126.
[12] Z.B. Wu, B.Q. Jiang, Y. Liu, W.R. Zhao, B.H. Guan, Experimental study on a low-temperature SCR catalyst based on MnO_x/TiO_2 prepared by sol–gel method, J. Hazard. Mater. 145 (2007) 488–494.
[13] M.M. Mohamed, I. Othmam, R.M. Mohamed, Synthesis and characterization of MnO_x/TiO_2 nanoparticles for photocatalytic oxidation of indigo carmin dye, J. Photochem. Photobiol. A 191 (2007) 153–161.
[14] N. Deb, A mechanistic approach on the solid state thermal decomposition of bimetallic oxalate coordination compounds of Mn(II), Fe(II) and Cu(II) with cobalt, J. Anal. Appl. Pyrolysis 78 (2007) 24–31.
[15] P. Yuan, X. Yin, H. He, D. Yang, L. Wang, J. Zhu, Investigation on the delaminated-pillared structure of TiO_2-PILC synthesized by $TiCl_4$ hydrolysis method, Microporous Mesoporous Mater. 93 (2006) 240–247.
[16] H. Yu, Q. Zhang, L. Qi, C. Lu, T. Xi, L. Luo, Thermal behavior of nitrided TiO_2/In_2O_3 by TG–DSC–MS combined with PulseTA, Thermochim. Acta 440 (2006) 195–199.
[17] P. Forzatti, Environmental catalysis for stationary applications, Catal. Today 62 (2000) 51–65.
[18] G. Carja, Y. Kameshima, K. Okada, C.D. Madhusoodana, Mn–Ce/ZSM5 as a new superior catalyst for NO reduction with NH_3, Appl. Catal. B 73 (2007) 60–64.
[19] C.L. Qin, J.J. Oak, N. Ohtsu, K. Asami, A. Inoue, XPS study on the surface films of a newly designed Ni-free Ti-based bulk metallic glass, Acta Mater. 55 (2007) 2057–2063.
[20] D.A. Pena, B.S. Uphade, E.P. Reddy, P.G. Smirniotis, Identification of surface species on titania-supported manganese, chromium, and copper oxide low-temperature SCR catalysts, J. Phys. Chem. B 108 (2004) 9927–9936.
[21] X. Tang, J. Hao, W. Xu, J. Li, Low temperature selective catalytic reduction of NO_x with NH_3 over amorphous MnO_x catalysts prepared by three methods, Catal. Commun. 8 (2007) 329–334.
[22] W.S. Kijlstra, M. Biervliet, E.K. Poels, A. Bliek, Deactivation by SO_2 of MnO_x/Al_2O_3 catalysts used for the selective catalytic reduction of NO with NH_3 at low temperatures, Appl. Catal. B 16 (1998) 327–337.
[23] G. Xie, Z. Liu, Z. Zhu, Q. Liu, J. Ge, Z. Huang, Simultaneous removal of SO_2 and NO_x from flue gas using a CuO/Al_2O_3 catalyst sorbent. I. deactivation of SCR activity by SO_2 at low temperatures, J. Catal. 224 (2004) 36–41.